Supporting information — Programmable aerosol chemistry coupled to chemical imaging establishes a new arena for automated chemical synthesis and discovery

Jakub D. Wosik, Chaoyi Zhu, Zehua Li, S. Hessam M. Mehr*

Materials and methods

Reagents

All reagents were purchased from Sigma–Aldrich and used without further purification. Specifications for the solutions used in our experiments can be found in **Table 1**. Reagent solutions used in the azo coupling experiment (bottom row) were combined fresh immediately prior to the experiment.

Table 1. Reagent solutions used in each experiment and their respective compositions.

Reaction	Reagent	Composition
Acid–base	**A:** Bromothymol blue (BTB, i.e. "acid")	0.05 BTB in 1:1 water–EtOH
	B: NaOH and phenolphthalein (PH)	0.05 M NaOH, 0.05 M PH in 1:1 EtOH
Redox	**A:** Ce^{4+} oxidiser	0.02 M aqueous $(NH_4)_2[Ce(NO_3)_6]$
	B: Reducing agent (Ferroin, Fe (II))	0.02 M aqueous $[Fe(Phen)_3]SO_4$
Azo coupling	**A:** Diazonium reagent (1 mL aniline solution + 2 mL HCl solution + 2 mL $NaNO_2$ solution)	**Aniline solution (aq):** 5.56 mg/mL, 0.06 M **HCl solution (aq):** 0.12 M **$NaNO_2$ solution (aq):** 0.08 M
	B: Sodium napthoxide solution (3 mL 2-naphthol solution + 2 mL NaOH solution)	**2-Napthol solution (aq):** 0.03 M **NaOH solution (aq):** 0.05 M

Optical microscopy

Microscopy measurements were carried out on an Olympus SZX7 microscope at 5.8x magnification using a Raspberry Pi HQ Camera for image acquisition. The camera was controlled via a connected Raspberry Pi 4B running Raspberry Pi operating system 11 (based on Debian 11 "Bullseye").

Software

The software library used to control piezoelectric driver circuit is *CtrlAer*, available under the MIT licence on GitHub (https://github.com/MehrResearch/ctrlaer), documented in a separate publication.[1]

Reagent module

The reagent module consists of a glass vial (Supelco SU860097) and metal screw cap (Supelco SU860102) purchased from Sigma–Aldrich and modified by removing the rubber septum and attaching a piezoelectric atomiser element (see below) to the cap using cyanoacrylate adhesive.

Atomiser element

The aerosol source used in this study is a piezoelectric vibrating mesh atomiser (VMA) widely available for domestic applications. Liquid droplets are extruded through a metal mesh of laser etched holes, in this case approximately 5 µm in diameter at the narrowest point, having a quoted resonance frequency of 110 kHz +/- 5%. An activation frequency of 113.5 kHz was used throughout our experiments.

Figure 1 shows a microscope image of the back side of the atomiser metal mesh. Laser drilled holes in this type of device are known to have a conical profile, their diameter widening significantly from front (ca. 5 µm) to back (ca. 12 µm).

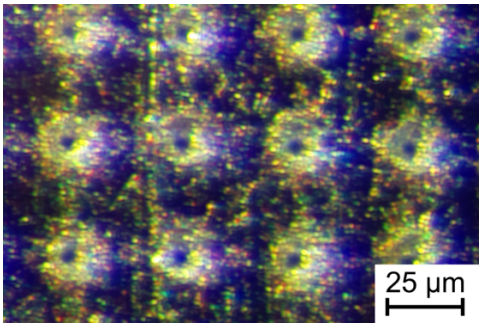

Figure 1. Microscope image of the vibrating mesh atomisers used in this study showing the metal .

AeroBoard

AeroBoard is an open-hardware system designed to allow automated, synchronised, multi-channel aerosol experiments using an intuitive Python-based programming interface. The GitHub repository provides Gerber files, bill of materials (BoM), and component placement files required for ordering a pre-assembled board.

Activating VMAs requires achieving resonance using a high-amplitude voltage signal. Common designs employ a compact autotransformer in conjunction with a MOSFET transistor in a flyback configuration to generate the voltage spikes required by the piezoelectric actuator. This design element is conserved in the AeroBoard, with additional direct visual feedback on activation provided by an LED to facilitate diagnosis.

We anticipate that the implementation of synthetic procedures as aerosol experiments will depend on a range of devices besides VMAs, such as valves, motors/actuators, and heating/cooling devices. The AeroBoard therefore includes four separate auxiliary channels dedicated to controlling devices with the same programming interface and level of precision. The inclusion of these four peripheral channels facilitates its incorporation into experiments where may need to be controlled in addition to VMA. Peripheral channel MOSFETs are each paired with a free-wheel diode for protection against voltage spikes originating from inductive loads.

Microdroplet collection and imaging

In our initial exploration, reaction outcomes were collected as microdroplets on the surface of a glass slide where, being dilute aqueous solutions, they are subject to rapid evaporation under ambient conditions. Observed under the microscope the residual solute from individual droplets can be seen as dark particles, making it impossible to register any colour. In order to reduce evaporation, a layer of oil was applied to the surface of the glass slide before starting the experiment to coat incoming the microdroplets. A high-

viscosity hydrophobic perfluoropolyether vacuum oil (Fomblin Y, ~6500 Da) was selected for its ability to preserve the spherical shape of solution microdroplets and minimize excessive spreading of the formation of blobs in our experiments. Once removed from the reactor, samples glass slides were immediately transferred to a custom moisture-saturated enclosure to prevent further evaporation, **Figure 2**. This clear enclosure can be assembled from laser cut acrylic sheets (CAD drawing available via OnShape). Being transparent, the entire assembly can be used for optical microscopy. In order to select representative sample areas for imaging and minimise bias, images were acquired "blind", i.e. random spots selected and acquired without looking at the contents.

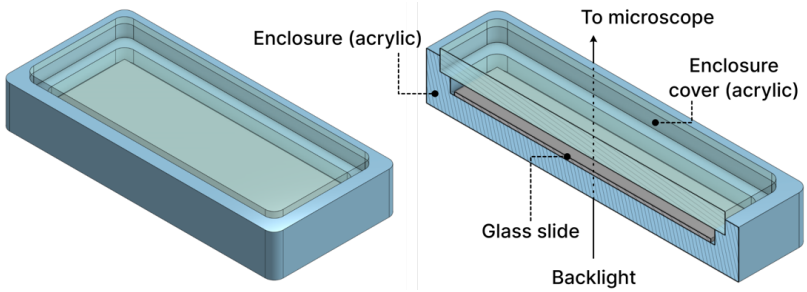

Figure 2. Acrylic enclosure used to minimize evaporation of collected microdroplets (left) and the slide–enclosure assembly as used for optical microscopy.

Image processing pipeline

Microscope images were first divided into segments using the Segment Anything model (SAM),[16] with the aim of assigning an image area, also known as region or segment, to each microdroplet in the sample image. As SAM is a general-purpose image segmentation model, some of the detected regions may belong to the background, empty space in between droplets, or other objects (dust particles). To remove these regions, a subsequent step was used to remove segments with area smaller than 25 μm^2 (dust or droplets too small to produce a discernible colour) or larger than 1500 μm^2 (background, halos, or spaces between particles detected as objects). Regions that deviate from a circular shape — calculated numerically as a *circularity* below 0.8 with 1 being a perfect circle — are also removed, **Figure 3**. All three limits can be fine-tuned within the Jupyter notebook.

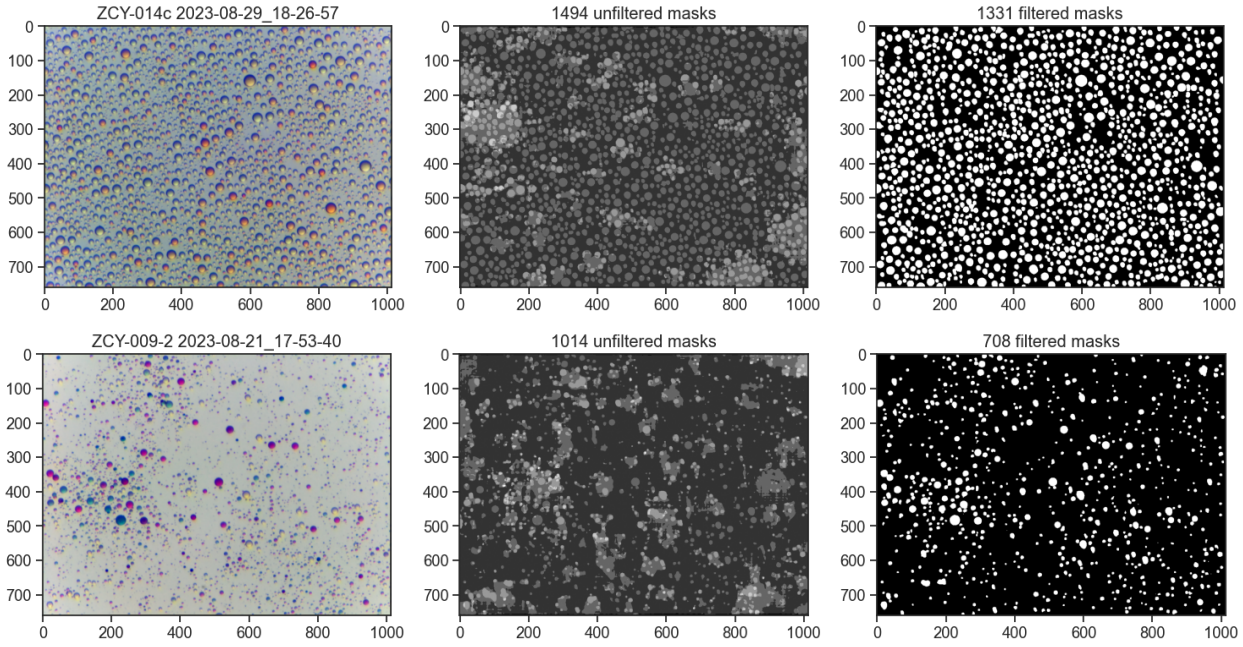

Figure 3. Post-processing of image regions for two exemplar microscope images.

Next, a representative RGB value was calculated to represent the colour of each droplet. We found that sampling from the centre of each droplet gave a realistic approximation of the droplet's perceived colour. Selecting the pixel with the maximum combined saturation and brightness value (S × V) gave comparable results, albeit with more saturated colours. Calculating the average RGB value over the entire droplet was also trialled; however, this average value did not reflect the perceived droplet colour due to the effect of bright spots and shadows caused by the droplet's lensing effect, **Figure 4**.

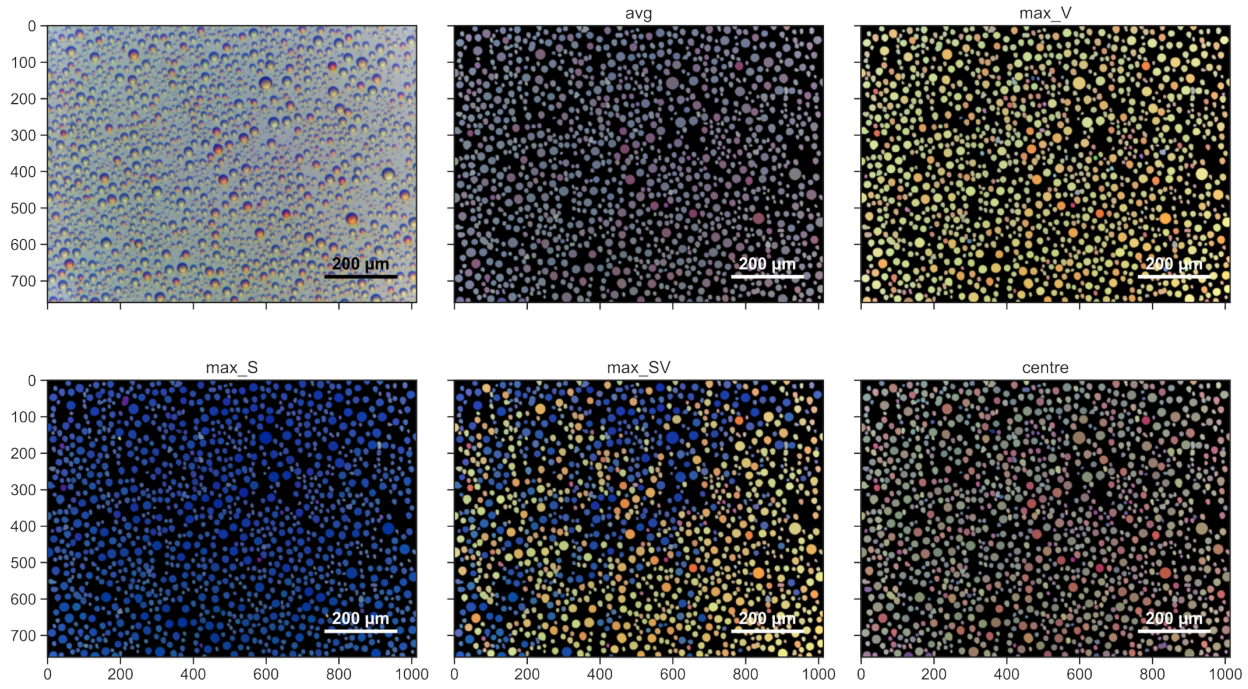

Figure 4. Comparison of five different criteria for assigning a representative colour to droplets: avg: RGB values averaged over the droplet area; max_V: the pixel with the highest brightness (value) in HSV colour space was chosen; max_S: the pixel with the highest saturation in HSV colour space was chosen; max_SV: the pixel with the highest product of saturation and value was chosen; centre: the pixel at the centre of the droplet was chosen.

In line with the inhomogeneous, stochastic nature of the experiment, there is variation in droplet size and count within the same sample, within images of the same experiment carried out on different dates, and between different experiments, **Figure 5**. Droplets, even when embedded in oil, are susceptible to evaporation, ripening, and motion under the Marangoni effect, introducing image acquisition time as another source of variability.

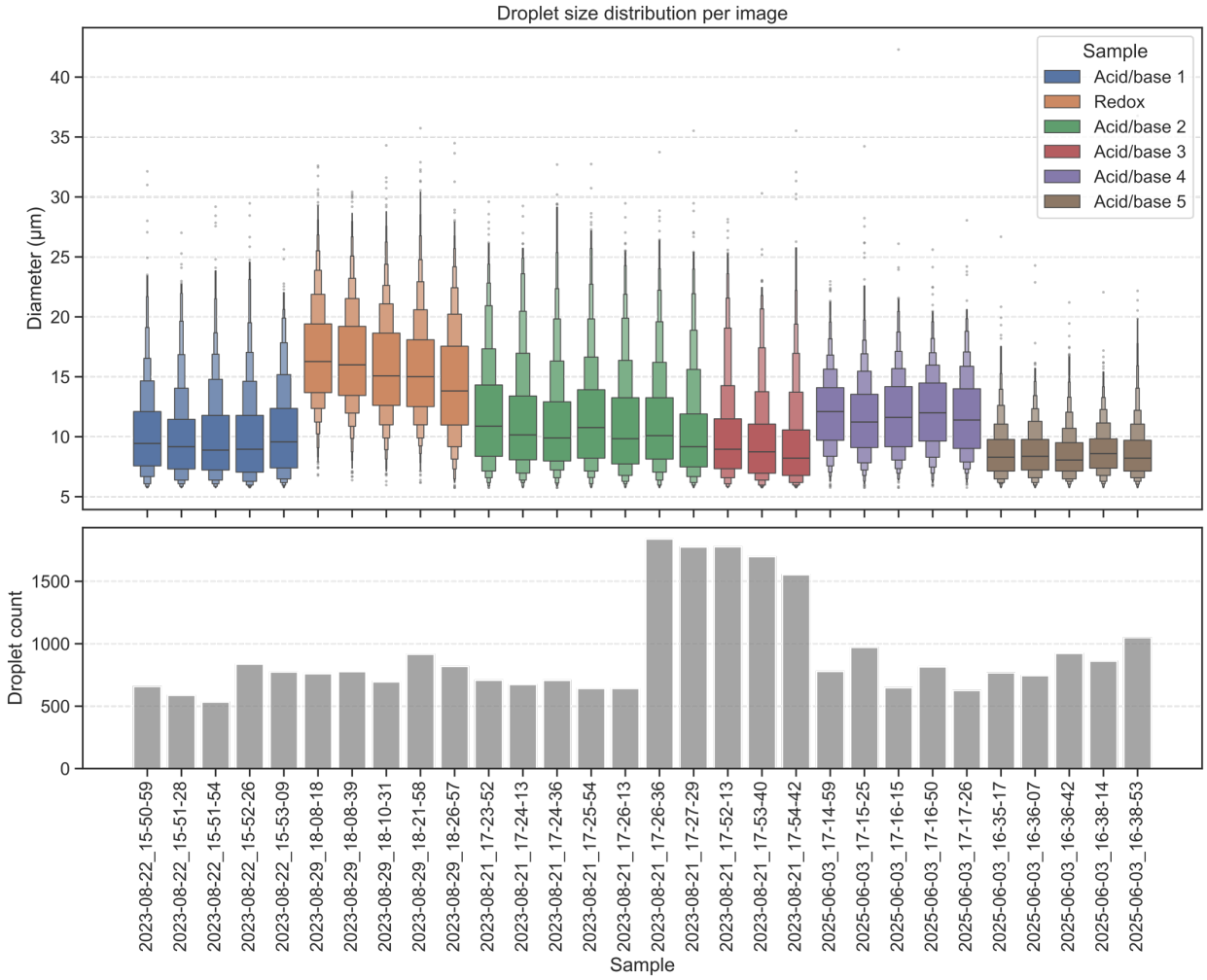

Figure 5. Comparison of droplet size distributions and counts across different images, colour-coded based on sample.

The distribution of RGB values in each image was fitted to a Gaussian Mixture model (GMM) in order to assign a composition to each droplet based on its color.[17] Using a GMM has the additional benefit of providing the degree of confidence for assigning droplets to colour clusters, equivalent to the likelihood of point in RGB space belonging to a three dimensional Gaussian distribution. We also tried to use colour coordinates in the HSV and LAB colour spaces, as well as relying only on hue values, i.e. distribution in a single dimension, to classify droplets, but found that the colour values are optimally segregated in the RGB space, **Figure 6**. Full computational details are available as a Jupyter notebook in the accompanying GitHub repository. Via this notebook, it is possible to specify any of the alternative spaces discussed above and compare the outcomes.

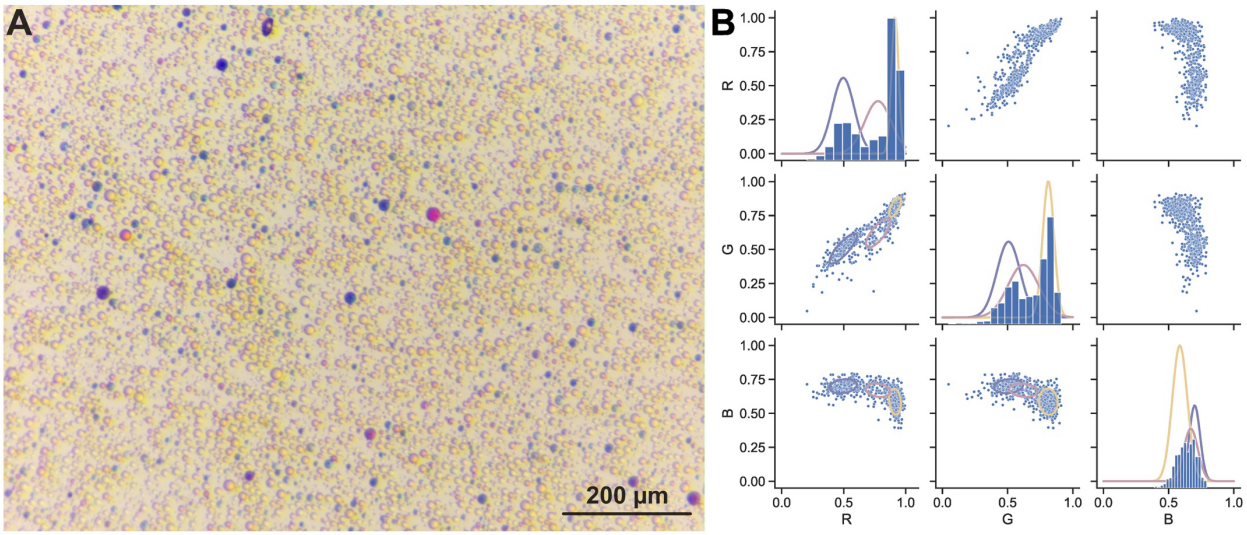

Figure 6. A: Optical microscope image of collected droplets in the reaction of acid-(yellow) and base-(purple) microdroplets with formation of product (blue) droplets. B: Distribution of droplet colours in RGB space as projections in the RG, RB, and GB planes. The distributions appear disjoint enough to assign most points to a cluster or centre with high probability.

The number of components in the GMM was set to 3, mirroring the expected binary reactivity with a single, coloured product: $A + B \rightarrow C$. Visualisation of the final droplets assigned to centres based on maximum likelihood conveniently followed this assumption, **Figure 7** and **Figure 8**.

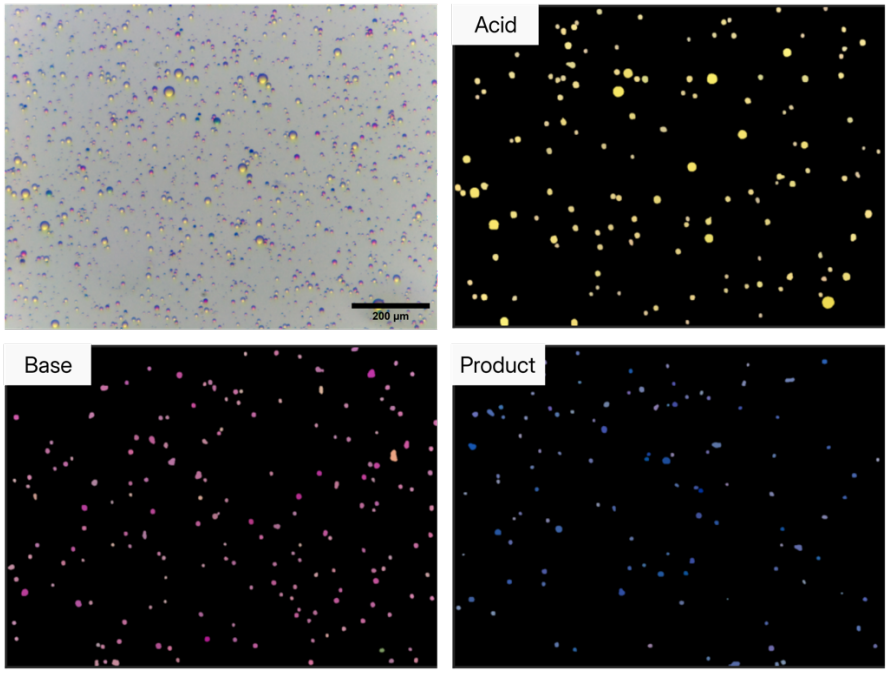

Figure 7. Optical microscope image of collected droplets in the reaction of acid-(yellow) and base-(purple) microdroplets with formation of product (blue) droplets. Categorization of droplets as acid, base or product (acid + base) using optical microscopy data.

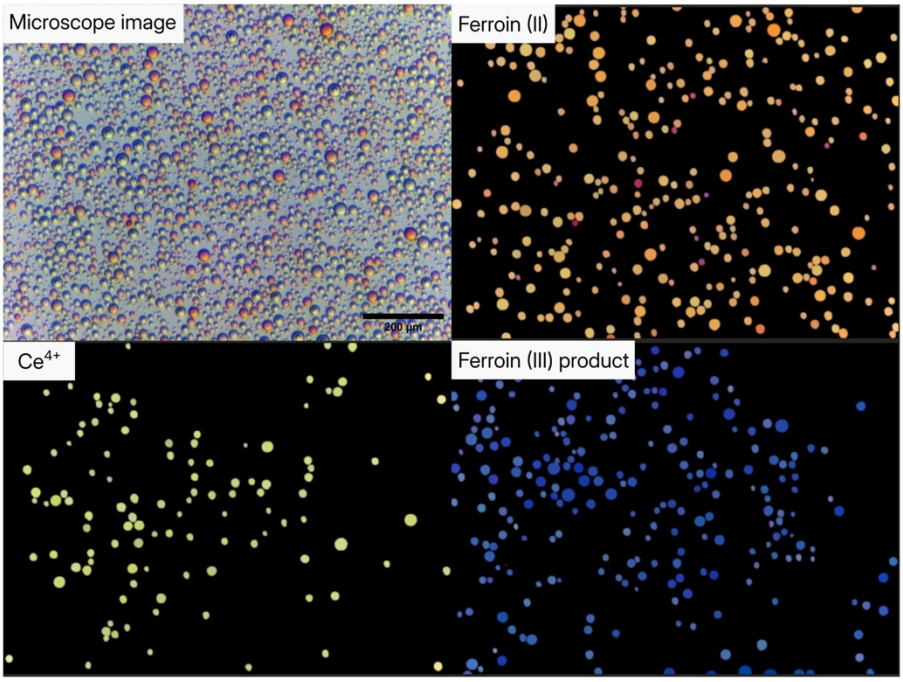

Figure 8. Microscope image taken from the glass slide for the redox reaction and three separated images based on the colour of the droplets.

Microscope image acquisition

The version of Raspberry Pi operating system used in this study supports the modern libcamera-based stack for interfacing with the imaging device, in this case a Raspberry Pi HQ camera. We created the convenience script in **Listing 1** for image acquisition which allows supplying an image prefix name, along with optional digital gain (directly related to the ISO number with 1.0 representing ISO 100) and shutter speed, which were not modified from their default values for the purpose of the images used in the present work.

```
#!/usr/bin/env bash

GAIN=${2:-1.0}
SHUTTER=${3:-250000}

rpicam-still -n -o "$1 $(date +%Y-%m-%d_%H-%M-%S).jpg" -q 100 --gain $GAIN --
shutter $SHUTTER --awbgains '3.4,1.6'
```

Listing 1. Command line used for image acquisition on the Raspberry Pi HQ camera.

LC–MS analysis of Sudan I synthesis outcome

As a qualitative validation of the Sudan I synthesis reaction using a non-colorimetric method, the product droplets from the reaction were collected via sedimentation in a 1 L wide-mouth glass Duran bottle. A small amount of the red powder deposit was dissolved in methanol, followed immediately with LC–MS analysis (Thermo UltiMate 3000 UHPLC, Bruker maxis impact mass spectrometer, C18 column, water/acetonitrile solvent gradient over 26 mins). Comparison of the resulting chromatogram with a commercial Sudan I

sample confirmed the presence of Sudan I ($C_{16}H_{12}N_2O$, peak 21 mins $[M+H]^+$ expected m/z 249.10279, observed in reaction mixture 249.1100, observed in commercial sample 249.0826), **Figure 9**.

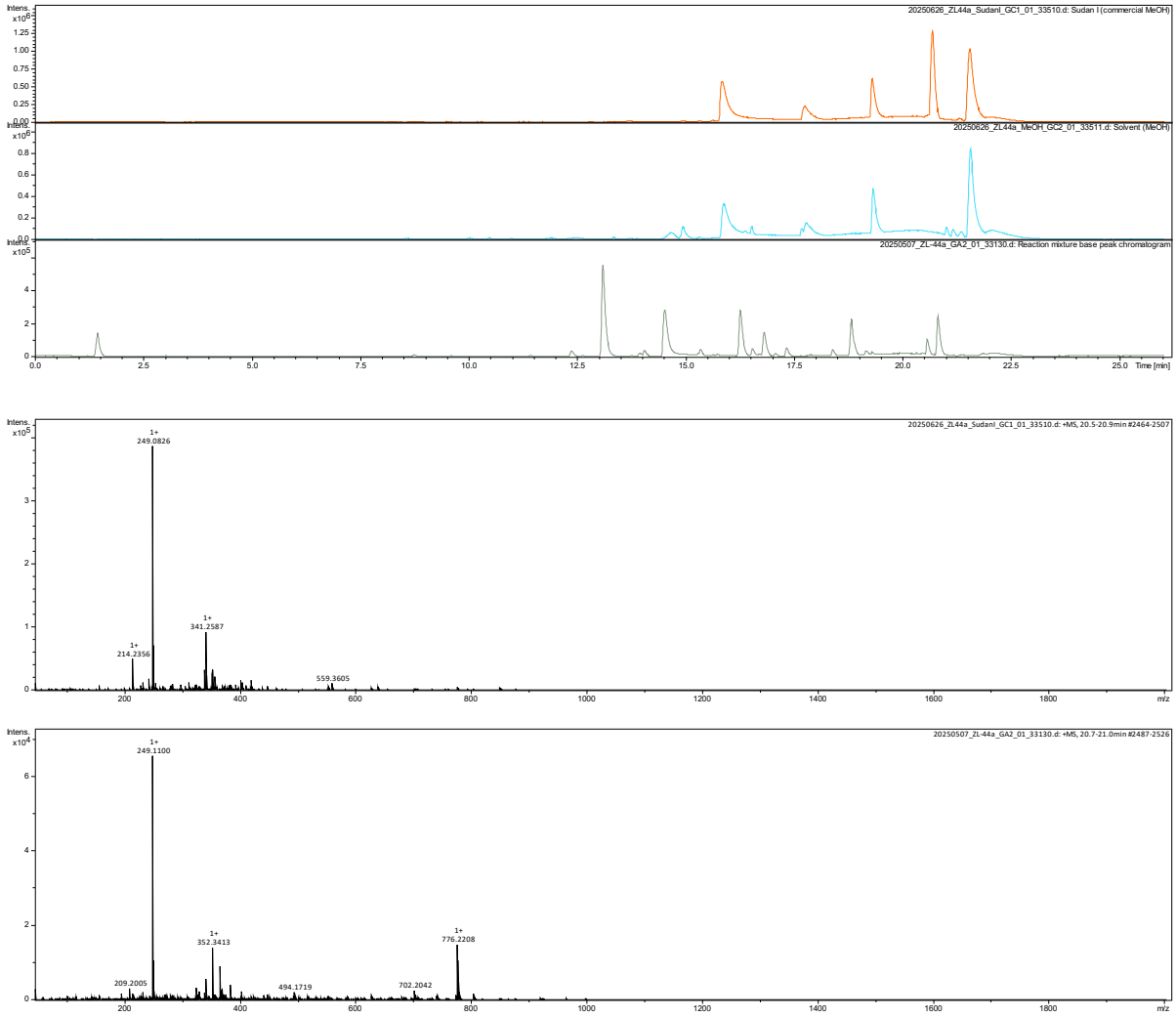

Figure 9. Bulk LC–MS analysis of reaction mixture from the synthesis of Sudan I following natural sedimentation of aerosol particles as a solid residue. Base peak chromatograms from top to bottom: commercial Sudan I dissolved in MeOH; MeOH solvent; reaction mixture dissolved in MeOH. Mass spectra from top to bottom: commercial Sudan I peak (20.5–20.9 min integrated); Sudan I in product mixture (20.7–21.0 min).

References

1. Mehr, S. H. M. CtrlAer: Programmable real-time execution of scientific experiments using a domain specific language for the Raspberry Pi Pico/Pico 2. *SoftwareX* **30**, 102175 (2025).